Physica A 202 (1994) 390–401
North-Holland

SSDI 0378-4371(93)E0402-Z

PHYSICA A

Numerical investigations of the evolution of sandpiles

Volkhard Buchholtz and Thorsten Pöschel

HLRZ, KFA Jülich, Postfach 1913, D-52425 Jülich, Germany
and Humboldt-Universität zu Berlin, FB Physik, Institut für Theoretische Physik, Invalidenstraße 42, D-10115 Berlin, Germany

Received 20 August 1993
Revised manuscript received 22 September 1993

The evolution of a pile of granular material is investigated by molecular dynamics using a new model including nonsphericity of the particles instead of introducing static friction terms. The angle of repose of the piles as well as the avalanche statistics gathered by the simulation agree with experimental results. The angle of repose of the pile is determined by the shape of the grains. Our results are compared with simulations using spherical grains and static friction.

1. Introduction

There are many interesting phenomena observed in the dynamics of granular materials which have been studied by many authors and by various methods (e.g. [1,2] and references therein). One of the most interesting phenomena is the evolution of a pile of granular material. When sand grains are dropped on the top of a pile its slope does not depend on the number of grains as long as the heap is not too small. The avalanches going down the surface of the heap have no characteristic size, they are only limited by the size of the entire pile. The size of the avalanches as well as the time interval between successive avalanches fluctuate irregularly. Their spectra decay possibly due to a power law [3–8]. On large scales, however, there was measured a different behaviour [9]. Recently Rosendahl et al. [3] found that the predominant number of avalanches is power law distributed but that these avalanches are supplemented by periodic significantly larger avalanches. Dependent on the material the slope of the surface of a heap can vary, hence one observes waves creeping up the pile [10].

There are different numerical methods to simulate the static and dynamic

behaviour of macroscopic amounts of granular media. Cundall and Strack [11] introduced a model for the interaction of grains which is widely used in molecular dynamics simulations. Other simulations base on cellular automata [12], and the results led to the idea of self-organized criticality [13]. Other numerical investigations base on the Boltzmann lattice gas [14], on Monte Carlo simulations (e.g. [15,16]) or on random walk models [17].

In this paper we apply a new model for the simulation of the evolution of sandpiles using molecular dynamics as introduced in [18]. Many of the numerical investigations base on molecular dynamics (e.g. [2,11,19–26]), however, most of them use spherical grains. To simulate static friction between the grains one introduces a force which is due to the Coulomb law, i.e. the spheres slide on each other for the case that the shear force between the grains F_S is larger than μF_N, where F_N is the force in normal direction, μ is the Coulomb friction coefficient. This friction force is derived from the phenomenological idea about friction between macroscopic bodies. Its microscopic origin is still hardly understood [27]. In our molecular dynamics simulations we use nonspherical particles instead of spheres. The particles we use here are elastic but not stiff, they deform during collisions and dissipate energy.

Recently Gallas and Sokołowski suggested a model for nonspherical grains where two spheres were connected by a stiff bar [28]. Their results agree qualitatively with ours.

As we will demonstrate below, the results of the simulations using nonspherical grains agree better with experimental investigations than traditional models.

2. The model

In our simulation each of the grains k consists of five spheres. Four of them, with radii $r_i^{(k)}$, are located at the corners of a square of size $L^{(k)}$. The fifth sphere is situated in the middle of the square and its radius is chosen to touch the others,

$$r_m^{(k)} = \frac{L^{(k)}}{\sqrt{2}} - r_i^{(k)} . \tag{1}$$

Each of the spheres is connected to all of its neighbouring spheres which belong to the same grain by damped springs (fig. 1).

Between each two spheres i and j which might belong to the same particle or to different particles acts the force $\boldsymbol{F}_{ij}$,

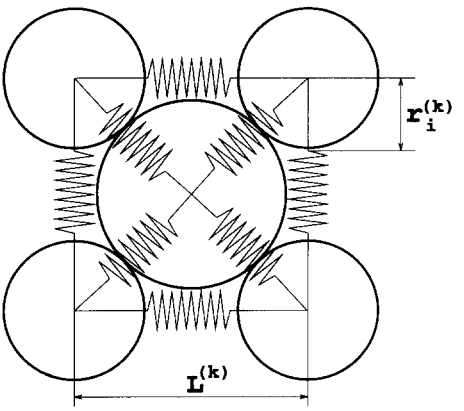

Fig. 1. Each of the particles k consists of four spheres with equal radii $r_i^{(k)}$ at the corners of a square of size $L^{(k)}$ and one sphere in the centre. Its radius is chosen to touch the others. There are forces due to a damped spring acting between the spheres the grain consists of.

$$\boldsymbol{F}_{ij} = \begin{cases} F_{ij}^{\mathrm{N}} \dfrac{\boldsymbol{x}_i - \boldsymbol{x}_j}{|\boldsymbol{x}_i - \boldsymbol{x}_j|}, & \text{if } |\boldsymbol{x}_i - \boldsymbol{x}_j| < r_i + r_j, \\ 0, & \text{otherwise}, \end{cases} \tag{2}$$

with the normal force

$$F_{ij}^{\mathrm{N}} = Y(r_i + r_j - |\boldsymbol{x}_i - \boldsymbol{x}_j|) - \gamma m_{ij}^{\mathrm{eff}} |\dot{\boldsymbol{x}}_i - \dot{\boldsymbol{x}}_j| \tag{3}$$

and the effective mass

$$m_{ij}^{\mathrm{eff}} = \frac{m_i m_j}{m_i + m_j}. \tag{4}$$

Y and γ are the Young modulus characterizing the elastic restoration of the spheres and the phenomenological damping coefficient. The terms $\boldsymbol{x}_i$, $\dot{\boldsymbol{x}}_i$ and m_i denote the current position, velocity and mass of the ith sphere. The normal force F_{ij}^{N} consists of an elastic restoration force which corresponds to the microscopic assumption that the particles can slightly deform each other and a term describing the energy dissipation of the system due to collisions between particles according to normal friction and plasticity.

Moreover each pair of neighbored spheres i and j which both belong to the same grain k feel the force

$$\boldsymbol{F}_{ij}^{\mathrm{Sp}} = [\alpha(C_{ij}^{(k)} - |\boldsymbol{x}_i - \boldsymbol{x}_j|) - \gamma_{\mathrm{Sp}}(m_i/2)|\dot{\boldsymbol{x}}_i - \dot{\boldsymbol{x}}_j|] \frac{\boldsymbol{x}_i - \boldsymbol{x}_j}{|\boldsymbol{x}_i - \boldsymbol{x}_j|}, \tag{5}$$

with

$$C_{ij}^{(k)} = \begin{cases} L^{(k)}, & \text{if } i, j \text{ lie at the same edge}, \\ L^{(k)}/\sqrt{2}, & \text{else}. \end{cases} \tag{6}$$

This force is due to internal damping with spring constant α and damping coefficient γ_{Sp} acting between particles of the same grain.

To compare our results using the nonspherical grains defined above we describe now how to introduce static friction in the simulation using spheres as it was done first by Cundall and Strack [11] and modified by Haff and Werner [19]. Here each pair of particles i and j with radii r_i and r_j feel the force

$$\boldsymbol{F}_{ij} = \begin{cases} F_{ij}^{\mathrm{N}} \dfrac{\boldsymbol{x}_i - \boldsymbol{x}_j}{|\boldsymbol{x}_i - \boldsymbol{x}_j|} + F_{ij}^{\mathrm{S}} \begin{pmatrix} 0 & -1 \\ 1 & 0 \end{pmatrix} \dfrac{\boldsymbol{x}_i - \boldsymbol{x}_j}{|\boldsymbol{x}_i - \boldsymbol{x}_j|}, & \text{if } |\boldsymbol{x}_i - \boldsymbol{x}_j| < r_i + r_j, \\ 0, & \text{otherwise}, \end{cases} \tag{7}$$

with the force in normal direction

$$F_{ij}^{\mathrm{N}} = Y(r_i + r_j - |\boldsymbol{x}_i - \boldsymbol{x}_j|) - \gamma m_{ij}^{\mathrm{eff}} |\dot{\boldsymbol{x}}_i - \dot{\boldsymbol{x}}_j| \tag{8}$$

and the shear force

$$F_{ij}^{\mathrm{S}} = \min(-\gamma_{\mathrm{S}} m_{ij}^{\mathrm{eff}} |\boldsymbol{v}_{ij}^{\mathrm{rel}}|, \mu |F_{ij}^{\mathrm{N}}|). \tag{9}$$

The relative velocity of the particle surfaces results from the relative velocity of the particles and their angular velocities $\dot{\Omega}_i$ and $\dot{\Omega}_j$

$$\boldsymbol{v}_{ij}^{\mathrm{rel}} = (\dot{\boldsymbol{x}}_i - \dot{\boldsymbol{x}}_j) + r_i \dot{\Omega}_i + r_j \dot{\Omega}_j. \tag{10}$$

The parameters γ and γ_{S} stand for the normal and shear friction coefficients, μ is the Coulomb friction parameter. Eq. (9) takes into account that two grains slide upon each other when the shear force between them exceeds a certain value, otherwise they roll (Coulomb relation).

The sizes of the nonspherical particles $L^{(k)}$ as well as the radii r_i in the case of spherical grains were Gauss distributed with mean value $\overline{L^{(k)}}$.

3. Results

In our simulation we investigate the evolution of a sand pile by consecutively dropping nonspherical particles on the top of the heap. The surface of the platform upon which the heap is built up consists of spheres with radii $r_i^{(\mathrm{p})}$ with

mean value $\overline{r_i^{(p)}} = \overline{L^{(k)}}$ to simulate a rough surface. After each dropping of a particle on the heap we waited until the velocities of all particles of the entire heap faded away, i.e. until they were smaller than a very small constant.

For the parameters we used in the simulations: $\underline{Y} = 10^4\ \mathrm{kg/s^2}$, $\gamma = 1.5 \times 10^4\ \mathrm{s^{-1}}$, $\alpha = 10^4\ \mathrm{kg/s^2}$, $\gamma_{\mathrm{Sp}} = 3 \times 10^4\ \mathrm{s^{-1}}$, $L^{(k)}/r_i^{(k)} = 4$, $\overline{L^{(k)}} = 3\ \mathrm{mm}$. The results were compared with simulations using spherical grains, where we assumed the same values and $\gamma_{\mathrm{S}} = 3 \times 10^4\ \mathrm{s^{-1}}$, $\mu = 0.5$ and $\overline{r_i} = 3\ \mathrm{mm}$.

For the calculation of the evolution of the particle positions we applied a Gear predictor corrector algorithm [29] of sixth order. For the case of the simulation using spherical grains we have further to calculate the rotation of each sphere. Since the acceleration of the particle surface due to particle rotation is much smaller than due to particle movement we applied therefore a Gear algorithm of fourth order only.

3.1. Angle of repose

When building up a heap experimentally one finds that the slope Φ (angle of repose) does not depend on the particle number. It depends on the raw material and lies typically between 20° and 30°. Bretz et al. found $\Phi \approx 25°$ [5].

Fig. 2 shows snapshots of simulated piles of different sizes. The size of the piles have been scaled so that the widths of all piles appear equal in the figures. The first two piles consist of $N = 300$ (fig. 2a) and $N = 1100$ (fig. 2b) nonspherical particles. The slope is approximately the same for both figures, i.e. it does not depend on the number of particles. Figs. 2c and 2d show piles of $N = 400$ and $N = 1800$ spherical particles. In the case of spherical grains the heap dissolves under gravity. The slope depends on the number of particles.

In the simulations using nonspherical grains we measured $\Phi \approx 21°$, this value is in agreement with experimentally found data [5]. Fig. 3 shows the evolution of the slope Φ of the pile during one run over the particle number for spherical and nonspherical grains. For nonspherical grains the slope Φ fluctuates due to avalanches of different size. Except for very small heaps the average slope does not depend on the particle number in accordance with the experiment. For the case of spherical particles the slope decays with rising particle number.

Since the surface of the pile is not a smooth line we need a special procedure to calculate the slope Φ. Fig. 4 shows a pile with an arbitrarily shaped heap. The shape of the pile is described by the function $h(x)$ with $x \in [0, x_{\max}]$, x_{cm} and y_{cm} denote the coordinates of the centre of mass of the heap. The height H of an ideal triangle which has the same baselength and volume like the heap would be

$$H = \frac{2}{x_{\max}} \int_0^{x_{\max}} h(x)\,\mathrm{d}x\,. \tag{11}$$

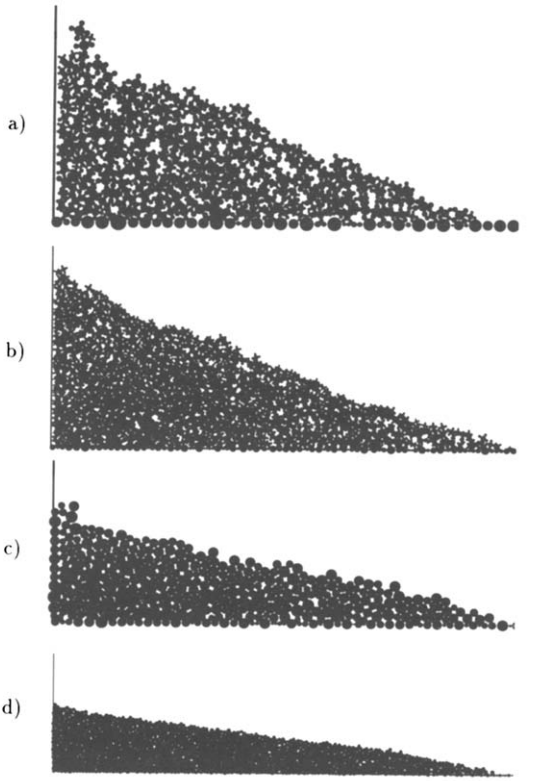

Fig. 2. Snapshots of simulated piles. Heaps (a) and (b) consist of $N = 300$ and $N = 1100$ nonspherical grains, heaps (c) and (d) of $N = 400$ and $N = 1800$ spherical particles. In the latter case the slope depends on the number of particles.

Because the centre of mass of a triangle is the intersection point of all three median lines we calculate the baselength B of the triangle using the intercept theorem

$$\frac{2H}{B} = \frac{H - y_{\mathrm{cm}}}{x_{\mathrm{cm}}} . \tag{12}$$

Hence we find for the slope

$$\Phi = \arctan\left(\frac{H - y_{\mathrm{cm}}}{2x_{\mathrm{cm}}}\right) . \tag{13}$$

Eq. (13) gives a good approximation for the slope provided that the shape of

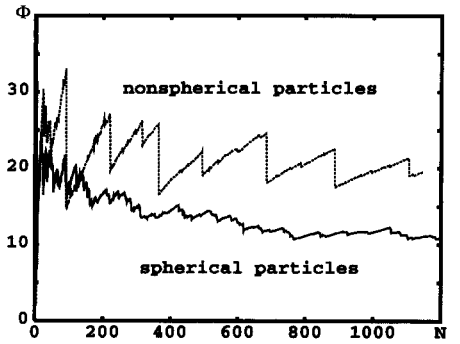

Fig. 4.

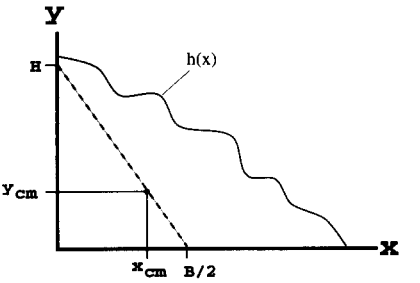

Fig. 3.

Fig. 3. The evolution of the slope of the pile during one run over the particle number for both spherical and nonspherical grains. For nonspherical grains the mean angle does not depend on the particle number while it decreases for spherical particles.

Fig. 4. Schematic plot of the procedure used to determine the slope of a pile which surface is not a smooth plane.

the heap is close to a triangle. The snapshots in fig. 2 show that this precondition is given in our case.

Notice that there are two possibilities of defining the angle [30], the angle of repose and the angle of marginal stability. For simplicity we used in this work the time average of the angle observed during the simulation.

3.2. *Avalanches and mass fluctuations*

Theoretical as well as experimental investigations [3–8,13] led to the hypothesis that the size of the avalanches, i.e. the mass fluctuations of the pile as well as the distribution of the time intervals between successive avalanches of sandpiles can be described by the self-organized criticality model. In order to investigate the size of the avalanches and the distribution of the time between each two successive avalanches we modified the setup of the simulation and monitor the fluctuation of the mass m_h of a heap of definite size. Instead of an infinite platform we use a platform of a finite length P above which the heap is built up. In fig. 5 is drawn a part of the time series of the mass m_h for fixed $P = 820\,\text{mm} \approx 273L^{(k)}$. The mass fluctuates irregularly due to avalanches of different size going down the surface of the heap. Since after dropping a grain on the heap we wait until the motion of all grains fades away the natural unit for measuring the time is the number of dropping events, but not the number of integration steps used in the simulation. Since we want to make statistics for all avalanches but not only for those which cause a change of

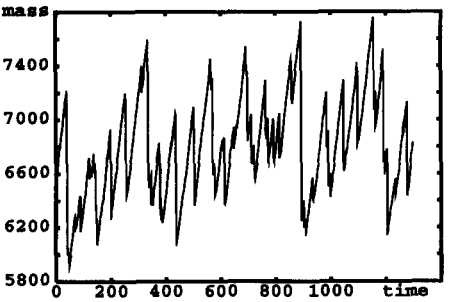

Fig. 5. Total mass of a pile of nonspherical grains on a platform of finite length $P = 820\,\text{mm} \approx 273\,L^{(k)}$. The mass fluctuates irregularly due to avalanches of different size. The time is measured in dropping events.

the mass m_h of the heap we monitor the change of the slope of the heap, i.e. the change of the centre of mass, during an avalanche instead of the change of the mass. Otherwise we would cut off the lower part of the spectrum since most of the small avalanches do not reach the bottom of the pile. Fig. 6 shows the time series of the avalanches. Fig. 6a displays the changes of the slope, fig. 6b the changes of the mass. Both figures resemble each other but in the latter case many of the small avalanches have been cut off. This is due to small avalanches which do not reach the bottom and therefore do not change the mass of the heap. The log–log plot of the spectrum (fig. 7) shows that the size distribution of the avalanches might follow a power law. For the exponent $h(N_A) \sim (N_A)^m$ we measured $m \approx -1.4$. In the experiments was found $m \approx -2.5$ [4] and $m \approx -2.134$ [5], respectively. The spectrum of the time intervals between each two successive avalanches was experimentally investigated too. Fig. 8 shows the spectrum of the distribution of the time intervals between two successive avalanches which we found in the simulation. We are not convinced that the decay of the spectrum in our simulation follows a power law too.

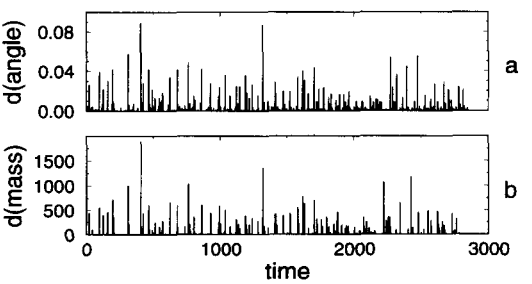

Fig. 6. Time series of the changes of the slope (a) and of the total mass (b) of the heap due to avalanches. Many of the small avalanches do not cause a change of the mass of the heap, since they stop before reaching the bottom.

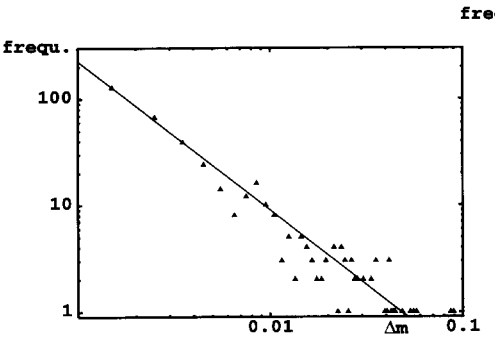

Fig. 8.

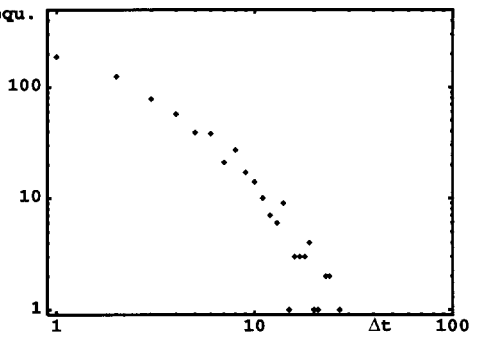

Fig. 7.

Fig. 7. Size distribution of the avalanches. The line displays the function $h(N_A) \sim (N_A)^{-1.4}$.

Fig. 8. Spectrum of the time intervals between successive avalanches.

3.3. *Influence of the particle sphericity*

Dependent on the ratio $L^{(k)}/r_i^{(k)}$ the grain k is more similar to a square or to a sphere. Hence we may investigate the influence of the particle shape on the angle of repose of a pile. We define the shape S of a grain

$$S = 1 - R^{cc}_{min}/R^{cc}_{max}\,, \tag{14}$$

where R^{cc}_{min} and R^{cc}_{max} are the extremal values of the distance between the convex cover of the nonspherical grain and its central point (fig. 9). In terms of $L^{(k)}/r_i^{(k)}$ we write

$$R^{cc}_{min} = \max\left(\frac{1}{\sqrt{2}}\frac{L^{(k)}}{r_i^{(k)}} - 1, \frac{1}{2}\frac{L^{(k)}}{r_i^{(k)}} + 1\right), \tag{15}$$

$$R^{cc}_{max} = \frac{1}{\sqrt{2}}\frac{L^{(k)}}{r_i^{(k)}} + 1\,. \tag{16}$$

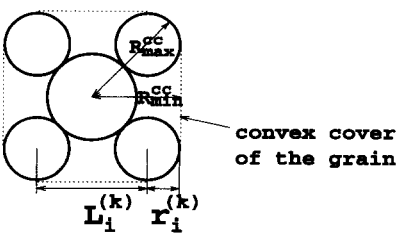

Fig. 9. The shape S is determined by the extreme sizes of the convex cover of the grains R^{cc}_{min} and R^{cc}_{max}.

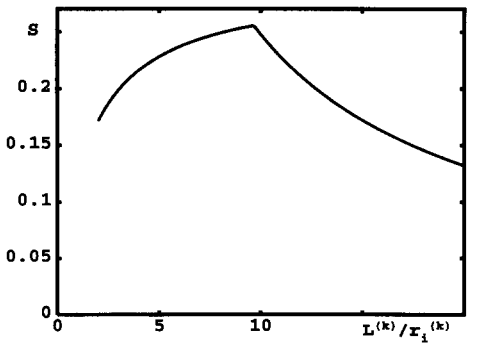

Fig. 11.

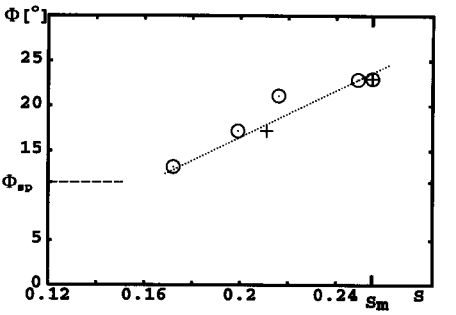

Fig. 10.

Fig. 10. The shape value S as a function of $L^{(k)}/r_i^{(k)}$. Each value S with $S < S_m$ corresponds to two different particle shapes with the same shape value, one with lower and one with larger $L^{(k)}/r_i^{(k)}$ ratio.

Fig. 11. Slope Φ of a heap over the shape value S for grains with $L^{(k)}/r_k^{(i)} \leqslant (L^{(k)}/r_i^{(k)})_{S_m}$ ($\odot$) and $L^{(k)}/r_i^{(k)} \geqslant (L^{(k)}/r_i^{(k)})_{S_m}$ (+). The dotted line leads the eye to the function $\Phi = 130S + \text{const}$. The dashed line displays the inclination observed in simulations with spherical particles.

Fig. 10 displays the shape value S as a function of $L^{(k)}/r_i^{(k)}$. The function S reaches its maximum S_m for a particle which convex cover is most similar to a square ($(L^{(k)}/r_i^{(k)})_{S_m} = 9.66$). For each $S < S_m$ there are two different particle shapes with the same shape value. Since $L^{(k)}/r_i^{(k)} \geqslant 2$ there are no particles with $S < 0.172$ for lower $L^{(k)}/r_i^{(k)}$ ratio. For the limit $L^{(k)}/r_i^{(k)} \to \infty$ the grains are spheres and S becomes zero.

To investigate the influence of the shape S of the grains on the result of the simulations we have to scale the density of the material the grains consist of to ensure that the total mass $m^{(k)}$ of each grain remains constant, independent of its shape ($\rho_0 \to \rho$ when $S_0 \to S$, $L^{(k)} = \text{const.}$, $m^{(k)} = \text{const.}$),

$$\rho(S) = \begin{cases} \rho_0 \dfrac{(2-S)^2}{(2-S_0)^2} \dfrac{4S_0^2 - 4S_0 + 2}{4S^2 - 4S + 2}, & \text{for } \dfrac{L^{(k)}}{r_i^{(k)}} \geqslant \left(\dfrac{L^{(k)}}{r_i^{(k)}}\right)_{S_m}, \\ \rho_0 \dfrac{4S^2}{4S_0^2} \dfrac{16S_0^2 + (12\sqrt{2} - 24)S_0 + 15 - 10\sqrt{2}}{16S^2 + (12\sqrt{2} - 24)S + 15 - 10\sqrt{2}}, & \text{for } \dfrac{L^{(k)}}{r_i^{(k)}} \leqslant \left(\dfrac{L^{(k)}}{r_i^{(k)}}\right)_{S_m}. \end{cases} \tag{17}$$

The influence of the shape of the grains on the slope of the heap is drawn in fig. 11. As mentioned above each S corresponds to two arguments $L^{(k)}/r_i^{(k)}$. Therefore we denote the slope for grains with $L^{(k)}/r_i^{(k)} \leqslant (L^{(k)}/r_i^{(k)})_{S_m}$ by $\odot$ and by + for $L^{(k)}/r_i^{(k)} \geqslant (L^{(k)}/r_i^{(k)})_{S_m}$. As expected the slope Φ reaches its maximum for particles with maximum shape value $S = S_m$ since they are most

similar to squares. The dashed line marks the inclination Φ_{Sp} we found for a heap of spheres, which corresponds to $S \to 0$. The slope values we measured simulating nonspherical grains lie between the slope of a pile of spheres and a pile of grains with $S = S_m$.

The calculation for the data shown in fig. 11 are extremely time consuming. For this reason we are not able to present more data.

4. Conclusion

Using molecular dynamics simulations we investigated the evolution of a sand pile and the statistics of the avalanches going down. Simulated piles using nonspherical grains remain stable under gravity; independent on their size the slope is approximately the same. In the simulation we found for the average slope $\overline{\Phi} \approx 13° \cdots 23°$ dependent on the shape of the grains. In experiments was found $\overline{\Phi} \approx 25°$ [5]. For the case of simulations using spheres and friction forces due to the Coulomb law the slope of the heap decreases with increasing particle number.

During the simulation the mass of the heap which is built up upon a finite platform varies irregularly. For the statistics of the avalanches we used the fluctuations of the slope of the heap, using the fluctuations of the mass leads to wrong results since most of the small avalanches do not reach the bottom of the heap and therefore do not change its mass. In our simulations the avalanches are power law distributed; for the exponent we found $h(N_A) \sim (N_A)^{-1.4}$.

Our model allows for changing the shape of the grains. We investigated the influence of their shape on the slope of the heap of constant size. We found that the slope reaches its maximum for grains which convex cover is most similar to a square. The minimum slope appears for the case that the particles are spheres. The slope of piles built of other nonspherical particles lies between the minimum and the maximum.

Acknowledgement

We thank J.A.C. Gallas and H.J. Herrmann for helpful discussions.

References

[1] H.M. Jaeger and S. Nagel, Science 255 (1992) 1523.
[2] H.J. Herrmann, Physica A 191 (1992) 263.

[3] J. Rosendahl, M. Vekić and J. Kelly, Phys. Rev. E 47 (1993) 1401.
[4] G.A. Held, D.H. Solina, D.T. Keane, W.J. Haag, P.M. Horn and G. Grinstein, Phys. Rev. Lett. 65 (1990) 1120.
[5] M. Bretz, J.B. Cunningham, P.L. Kurczynski and F. Nori, Phys. Rev. Lett. 69 (1992) 2431.
[6] D. Dhar, Phys. Rev. Lett. 64 (1990) 1613.
[7] B. McNamara and K. Wiesenfeld, Phys. Rev. A 41 (1990) 1867.
[8] L.P. Kadanoff, S.R. Nagel, L. Wu and S. Zhou, Phys. Rev. A 39 (1989) 6524.
[9] H.M. Jaeger, C. Liu and S. Nagel, Phys. Rev. Lett. 62 (1989) 40.
[10] V. Frette, Phys. Rev. Lett. 70 (1993) 2762.
[11] P. Cundall and O.D.L. Strack, Géotechnique 29 (1979) 47.
[12] G.W. Baxter and R.P. Behringer, Phys. Rev. A 42 (1990) 1017.
[13] P. Bak, C. Tang and K. Wiesenfeld, Phys. Rev. Lett. 59 (1987) 381.
[14] E. Flekkøy and H.J. Herrmann, preprint HLRZ (1993).
[15] P. Devillard, J. Phys. (France) 51 (1990) 369.
[16] A. Rosato, K.J. Strandburg, F. Prinz and R.H. Swendsen, Phys. Rev. Lett. 58 (1987) 1038.
[17] H. Caram and D.C. Hong, Phys. Rev. Lett. 67 (1991) 828.
[18] T. Pöschel and V. Buchholtz, preprint HLRZ 33-93 (1993).
[19] P.K. Haff and B.T. Werner, Powder Technol. 48 (1986) 239.
[20] P.A. Thompson and G.S. Grest, Phys. Rev. Lett. 67 (1991) 1751.
[21] T. Ohtsuki, Y. Takemoto and A. Hayashi, preprint.
[22] J.A.C. Gallas, H.J. Herrmann and S. Sokołowski, Phys. Rev. Lett. 69 (1992) 1371.
[23] Y.H. Taguchi, Phys. Rev. Lett. 69 (1992) 1367.
[24] G. Ristow, J. Phys. (France) 2 (1991) 649.
[25] D.C. Hong and J.A. McLennan, Physica A 187 (1992) 159.
[26] T. Pöschel, J. Phys. (France) 3 (1993) 27; preprint HLRZ 67-92 (1992).
[27] T. Pöschel and H.J. Herrmann, Physica A 198 (1993) 441.
[28] J.A.C. Gallas and S. Sokołowski, Int. J. Mod. Phys. B 7 (1993) 2037.
[29] M.P. Allen and D.J. Tildesley, Computer Simulations of Liquids (Clarendon Press, Oxford, 1987);
O.R. Walton and R.L. Braun, J. Rheol. 30 (1986) 949.
[30] J. Lee, preprint HLRZ 71-92 (1992).